

# NMRlipids IV: Headgroup & glycerol backbone structures, and cation binding in bilayers with PS lipids

Pavel Buslaev,<sup>1</sup> Tiago M. Ferreira,<sup>2</sup> Ivan Gushchin,<sup>1</sup> Matti Javanainen,<sup>3</sup> Batuhan Kav,<sup>4</sup> Jesper J. Madsen,<sup>5</sup> Markus Miettinen,<sup>4</sup> Josef Melcr,<sup>3</sup> Ricky Nencini,<sup>3</sup> O. H. Samuli Ollila,<sup>3,6,\*</sup> and Thomas Piggot **1.Authorlist is not yet complete**<sup>7</sup>

<sup>1</sup>*Moscow Institute of Physics and Technology*

<sup>2</sup>*Halle, Germany*

<sup>3</sup>*Institute of Organic Chemistry and Biochemistry, Academy of Sciences of the Czech Republic, Prague 6, Czech Republic*

<sup>4</sup>*Potsdam, Germany*

<sup>5</sup>*Department of Chemistry, The University of Chicago, Chicago, Illinois 60637, United States of America*

<sup>6</sup>*Institute of Biotechnology, University of Helsinki*

<sup>7</sup>*Southampton, United Kingdom*

(Dated: November 20, 2018)

Phosphatidylserine (PS) is the most common negatively charged lipid in eukaryotic membranes. PS lipids interact with signaling and other proteins via electrostatic interactions and direct binding, and induce membrane fusion and phase separation together with calcium ions. Molecular details of these phenomena are not well understood because accurate models to interpret the experimental data has not been available. Here, we collect a set of experimental NMR data which could be used together with molecular dynamics (MD) simulations to interpret the lipid headgroup structures and details of ion binding in pure and mixed PS and PS:PC lipid bilayers. Aiming to interpret the data, we use the open collaboration method to go through the available MD simulation models for PS lipids. However, none of the models reproduce the experimental data with sufficient accuracy to interpret the structural details of lipid headgroups or ion binding details in lipid bilayers containing PS lipids. In contrast to PC lipids, the tested MD simulation models do not correctly reproduce the qualitative response of PS lipid headgroups to the bound ions or changes in the lipid composition. Our results pave the way for the model improvement to correctly describe negatively charged membranes and their interactions with ions.

## INTRODUCTION

Phosphatidylserine (PS) is the most common negatively charged lipid in eukaryotic membranes. PS lipids compose 8.5% of total lipid weight of erythrocytes, but the abundance varies between different organelles up to 25-35% in plasma membrane [1–3]. Despite of the relatively low abundance, PS lipids are important signaling molecules. They interact with signaling proteins [2], regulate surface charge and protein localization [4], and induce protein aggregation [5, 6]. Some domains specifically interact PS lipids, while others are attracted by general electrostatics and the binding can be regulated by calcium [2]. Therefore, the structural details of lipid headgroups and the details of cation binding are crucial for the PS mediated signaling processes.

Previous experimental studies have concluded that PS headgroups are more rigid than phosphocholines (PC) due to the hydrogen bonding network or electrostatic interactions [7, 8]. Multivalent cations and  $\text{Li}^+$  are able to form strong dehydrated molecular complexes with PS lipids, while monovalent ions interact more weakly with PS containing bilayers [9–19]. The dehydrated complexes of PS headgroup and calcium ions can also lead to the phase separation [9, 10, 14–18]. On the other hand, some studies propose that the specific binding affinity is similar to the negatively charged and zwitterionic lipids and that the increased cation binding to negatively charged lipid bilayer arise only due to the increase of local cation concentration in the vicinity of membranes [20, 21]. Dilution of bilayers with PC lipids makes PS headgroups less rigid and reduces propensity for the formation of strong com-

plexes with multivalent ions [7, 8, 17, 18]. The molecular level interpretation of these observations is, however, not available.

Several classical molecular dynamics (MD) simulation studies are done to understand PS headgroups, their influence on lipid bilayer properties and interactions with ions [19, 22–32]. However, the recent comparisons of PC lipid headgroup and glycerol backbone C-H bond order parameters calculated from different simulation models revealed that improvements in the current force fields are needed to correctly reproduce the headgroup structure and ion binding to lipid bilayers [33–35]. The ion binding affinity to POPC bilayer was then improved by implicitly including the electronic polarizability using the electronic continuum correction [36]. Here, we collect the set of experimentally measured lipid headgroup and glycerol backbone C-H bond order parameters, which can be used to evaluate the quality of headgroup structure and the ion binding affinity in MD simulations of lipid bilayers containing PS lipids. The available MD simulation models of PS are then compared against the collected experimental data. The results pave the way for the development of MD simulation force fields that correctly describe PS lipid headgroup structure and its interactions with ions. Such models are expected to be useful in elucidating the biological role of PS and other lipid headgroups because glycerol backbone and lipid headgroups behave similarly in model membranes and in bacteria [20, 37, 38].

TABLE I: List of MD simulations of pure PS bilayers without additional salt. CKPM refers to the version with Berger/Chiu  $\text{NH}_3$  charges compatible with Berger (i.e. the  $\text{NH}_3$  group having the same charges as in the  $\text{N}(\text{CH}_3)_3$  group of the PC lipids; 'M' stands for Mukhopadhyay after the first published Berger-based PS simulation that used these charges [24]) and CKP refers to the version with more Gromos compatible version (i.e. the charges for the  $\text{NH}_3$  group taken from the lysine side-chain).

lipid/counter-ions	force field for lipids / ions	$^a\text{N}_l$	$^b\text{N}_w$	$^c\text{N}_c$	$^d\text{T (K)}$	$^e t_{\text{sim}}(\text{ns})$	$^f t_{\text{anal}}(\text{ns})$	$^g \text{files}$
DOPS/ $\text{Na}^+$	CHARMM36 [29]	128	4480	0	303	500	100	[39]
DOPS/ $\text{Na}^+$	CHARMM36ua [?] ] 2.	128	4480	0	303	500	100	[40]
DOPS/ $\text{Na}^+$	Slipids [41]	128	4480	0	303	500	100	[42]
DOPS/ $\text{Na}^+$	Slipids [41]	288	11232	0	303	200	100	[43]
DOPS/ $\text{Na}^+$	Berger [24]	128	4480	0	303	500	100	[44]
DOPS/ $\text{Na}^+$	GROMOS-CKPM [?] ] 3.	128	4480	0	303	500	100	[45]
DOPS/ $\text{Na}^+$	GROMOS-CKP [?] ] 4.	128	4480	0	303	500	100	[46]
DOPS/ $\text{Na}^+$	lipid17 [47] / JC [48]	128	4480	0	303	600	100	[49]
DOPS/ $\text{Na}^+$	lipid17 [47] / ff99 [50]	128	4480	0	303	600	100	[51]
POPS/ $\text{Na}^+$	CHARMM36 [29]	128	4480	0	298	500	100	[52]
POPS/ $\text{K}^+$	CHARMM36 [29]	128	4480	0	298	500	100	[53]
POPS/ $\text{Na}^+$	CHARMM36ua [?] ] 5.	128	4480	0	298	500	100	[54]
POPS/ $\text{Na}^+$	Slipids [41]	128	4480	0	298	500	100	[55]
POPS/ $\text{Na}^+$	Berger [?] ]	128	4480	0	298	500	100	[56]
POPS/ $\text{Na}^+$	MacRog [57]	128	4480	0	298	500	100	[58]
POPS/ $\text{K}^+$	MacRog [57]	128	4480	0	298	200	150	[?] ]
POPS/ $\text{Na}^+$	GROMOS-CKPM [?] ] 6.	128	4480	0	298	500	100	[60]
POPS/ $\text{Na}^+$	GROMOS-CKP [?] ] 7.	128	4480	0	298	500	100	[61]
POPS/ $\text{Na}^+$	lipid17 [47] / JC [48]	128	4480	0	298	600	100	[62]
POPS/ $\text{Na}^+$	lipid17 [47] / ff99 [50]	128	4480	0	298	600	100	[63]

<sup>a</sup>Number of lipid molecules with largest mole fraction

<sup>b</sup>Number of water molecules

<sup>c</sup>Number of additional cations

<sup>d</sup>Simulation temperature

<sup>e</sup>Total simulation time

<sup>f</sup>Time used for analysis

<sup>g</sup>Reference for simulation files

## METHODS

### Solid state NMR experiments

Headgroup and glycerol backbone C-H bond order parameters of POPS were determined from chemical-shift resolved dipolar splittings measured with a R-type Proton Detected Local Field (R-PDFL) experiment [82] and corresponding order parameter signs were measured with a S-DROSS experiment [83] using natural abundance  $^{13}\text{C}$  solid state NMR spectroscopy as described previously [84, 85]. The experiments were done in a Bruker Avance III 400 spectrometer operating at a  $^1\text{H}$  Larmor frequency of 400.03 MHz. Magic angle spinning (MAS) of the sample was used at a frequency of 5.15 kHz (R-PDFL experiment) and 5 kHz (S-DROSS experiment). The following experimental setups were used.

**R-PDFL experiment.** The parameters are described according to Figures 1c and 2c of the original reference for the R-PDFL experiment [82]. The refocused-INEPT delays  $\tau_1$  and  $\tau_2$  were 1.94 ms and 0.97 ms, respectively. Radio fre-

quency pulses with the nutation frequencies: 46.35 kHz ( $\text{R18}_1^7$  pulses), 63.45 kHz ( $^{13}\text{C}$   $90^\circ$  and  $180^\circ$ ), 50 kHz (SPINAL64  $^1\text{H}$  decoupling pulses). The  $t_1$  increment was equal to  $10.79 \mu\text{s} \times 18 \times 2$  and 32 points in the indirect dimension were recorded using 1024 scans for each, with recycle delay of 5 s and a spectral width of 149.5 ppm.

**S-DROSS experiment.** The parameters are described according to Figures 1b and 1c of the original reference for the S-DROSS experiment [83]. The refocused-INEPT delay  $\delta_2$  was 1.19 ms. The  $\tau_1$  and  $\tau_2$  in the S-DROSS recoupling blocks  $R$  were set as  $39.4 \mu\text{s}$  and  $89.4 \mu\text{s}$ , respectively. Radio frequency pulses with the nutation frequencies: 63.45 kHz ( $^{13}\text{C}$   $90^\circ$  and  $180^\circ$ ), 50 kHz ( $^1\text{H}$  SPINAL64 decoupling). The  $t_1$  increment (dipolar recoupling dimension) was  $800 \mu\text{s}$  and a total of 8 points along  $t_1$  were measured using 1024 scans for each with a recycle delay of 5 s and a spectral width of 149.5 ppm.

**NMR numerical simulations** The numerical simulations of S-DROSS curves were performed with the SIMPSON simulation package [86] using the  $^{13}\text{C}$ - $^1\text{H}$  dipolar couplings de-

TABLE II: List of POPC:POPS mixture simulations with different amounts of added ions. The salt concentrations calculated as  $[\text{salt}] = N_c \times [\text{water}] / N_w$ , where  $[\text{water}] = 55.5 \text{ M}$ . these correspond the concentrations reported in the experiments by Roux et al. [17].

lipid/counter-ions	force field for lipids / ions	$^a C_{ci} \text{ (M)}$	$[\text{CaCl}_2] \text{ (M)}$	$^b N_l$	$^c N_w$	$^d N_c$	$^e T \text{ (K)}$	$^f t_{\text{sim}} \text{ (ns)}$	$^g t_{\text{anal}} \text{ (ns)}$	$^h \text{files}$
POPC:POPS (5:1)/K <sup>+</sup>	CHARMM36 [29, 64]	0	0	110:22	4935	0	298	100	100 <b>8.</b>	[65]
POPC:POPS (5:1)/K <sup>+</sup>	CHARMM36 [29, 64]	0	0	250:50	?	0	298	200	?	[?] <b>9.</b>
POPC:POPS (5:1)/K <sup>+</sup>	CHARMM36 [29, 64]	0	0	110:22	4620	0	298	500	100	[66]
POPC:POPS (5:1)/K <sup>+</sup>	CHARMM36 [29, 64]	0.45	0	110:22	4926	40	298	200	150	[?] ]
POPC:POPS (5:1)/K <sup>+</sup>	CHARMM36 [29, 64]	0.89	0	110:22	4946	79	298	200	150	[?] ]
POPC:POPS (5:1)/Na <sup>+</sup>	CHARMM36 [29, 64]	0	0	110:22	4620	0	298	500	100	[67]
POPC:POPS (5:1)/K <sup>+</sup>	CHARMM36 [29, 64]	0.44	0	110:22	4965	39	298	200	150	[?] ]
POPC:POPS (5:1)/K <sup>+</sup>	CHARMM36 [29, 64]	0.89	0	110:22	4932	79	298	200	150	[?] ]
POPC:POPS (5:1)	CHARMM36 [29, 64, 68]	0	0.15 <b>10.</b>	250:50	?	?	298	200	?	[?] ] <b>11.</b>
POPC:POPS (5:1)	CHARMM36 [29, 64, 68]	0	1 <b>12.</b>	250:50	?	?	298	200	?	[?] ] <b>13.</b>
POPC:POPS (1:1)/K <sup>+</sup>	CHARMM36 [29, 64]	0	0	150:150	?	0	298	200	?	[?] ] <b>14.</b>
POPC:POPS (5:1)/K <sup>+</sup>	MacRog [57]	0	0	120:24	5760	0	298	400	250	[69]
POPC:POPS (5:1)/K <sup>+</sup>	MacRog [57]	0	0.10	120:24	5760	10	298	600	300	[69]
POPC:POPS (5:1)/K <sup>+</sup>	MacRog [57]	0	0.30	120:24	5760	31	298	600	300	[69]
POPC:POPS (5:1)/K <sup>+</sup>	MacRog [57]	0	1.00	120:24	5760	104	298	600	300	[69]
POPC:POPS (5:1)/K <sup>+</sup>	MacRog [57]	0	3.00	120:24	5760	311	298	600	300	[69]
POPC:POPS (5:1)/K <sup>+</sup>	MacRog [57]	0.50	0	120:24	5760	52	298	300	200	[70]
POPC:POPS (5:1)/K <sup>+</sup>	MacRog [57]	1.00	0	120:24	5760	104	298	300	200	[70]
POPC:POPS (5:1)/K <sup>+</sup>	MacRog [57]	2.00	0	120:24	5760	208	298	300	200	[70]
POPC:POPS (5:1)/K <sup>+</sup>	MacRog [57]	3.00	0	120:24	5760	311	298	300	200	[70]
POPC:POPS (5:1)/K <sup>+</sup>	Lipid14/17 [47, 71]	0	0	120:24	5760	0	298	500	200	[72]
POPC:POPS (5:1)/K <sup>+</sup>	Lipid14/17 [47, 71]	0.5 <b>15.</b>	0	120:24	5760	?	298	300	200	[73]
POPC:POPS (5:1)/K <sup>+</sup>	Lipid14/17 [47, 71]	1 <b>16.</b>	0	120:24	5760	?	298	300	200	[73]
POPC:POPS (5:1)/K <sup>+</sup>	Lipid14/17 [47, 71]	2 <b>17.</b>	0	120:24	5760	?	298	300	200	[73]
POPC:POPS (5:1)/K <sup>+</sup>	Lipid14/17 [47, 71]	3 <b>18.</b>	0	120:24	5760	?	298	300	200	[73]
POPC:POPS (5:1)/K <sup>+</sup>	Lipid14/17 [47, 71]	4 <b>19.</b>	0	120:24	5760	?	298	300	200	[73]
POPC:POPS (5:1)/Na <sup>+</sup>	Lipid14/17 [47, 71]	0	0	120:24	5760	0	298	500	200	[74]
POPC:POPS (5:1)/Na <sup>+</sup>	Lipid14/17 [47, 71]	0.5 <b>20.</b>	0	120:24	5760	?	298	300	200	[75]
POPC:POPS (5:1)/Na <sup>+</sup>	Lipid14/17 [47, 71]	1 <b>21.</b>	0	120:24	5760	?	298	300	200	[75]
POPC:POPS (5:1)/Na <sup>+</sup>	Lipid14/17 [47, 71]	2 <b>22.</b>	0	120:24	5760	?	298	300	200	[75]
POPC:POPS (5:1)/Na <sup>+</sup>	Lipid14/17 [47, 71]	3 <b>23.</b>	0	120:24	5760	?	298	300	200	[75]
POPC:POPS (5:1)/Na <sup>+</sup>	Lipid14/17 [47, 71]	4 <b>24.</b>	0	120:24	5760	?	298	300	200	[75]
POPC:POPS (5:1)/Na <sup>+</sup>	Lipid14/17 [47, 71]	0	0	60:12	3600	0	298	1000	1000	[?] ]
POPC:POPS (5:1)/Na <sup>+</sup>	Lipid14/17 [47, 71]	0	0.08	60:12	3561	5	298	1000	1000	[?] ]
POPC:POPS (5:1)/Na <sup>+</sup>	Lipid14/17 [47, 71]	0	0.13	60:12	3561	8	298	1000	1000	[?] ]
POPC:POPS (5:1)/Na <sup>+</sup>	Lipid14/17 [47, 71]	0	0.20	60:12	3561	13	298	1000	1000	[?] ]
POPC:POPS (5:1)/Na <sup>+</sup>	Lipid14/17 [47, 71]	0	0.41	60:12	3522	26	298	1000	1000	[?] ]
POPC:POPS (5:1)/Na <sup>+</sup>	Lipid14/17 [47, 71]	0	0.62	60:12	3483	39	298	1000	1000	[?] ]
POPC:POPS (4:1)/Na <sup>+</sup>	Berger [24, 76]	0	0	102:26	4290	0	310	80	120	[?] ]
POPC:POPS (4:1)/Na <sup>+</sup>	Berger [24, 76] <b>25.</b>	1.03	0	102:26	4290	80	310	200	50	[77]
POPC:POPS (4:1)	Berger [24, 76]	0	0.12 <sup>i</sup>	104:24	4306	24	310	300	100	[78]
POPC:POPS (4:1)	Berger [24, 76]	0	0.715 <sup>j</sup>	104:24	4306	72	310	300	100	[79]
POPC:POPS (5:1)/Na <sup>+</sup>	GROMOS-CKP [?] ]	0	0	110:22	?	0	298	500	100	[80]
POPC:POPS (5:1)/Na <sup>+</sup>	GROMOS-CKPM [?] ]	0	0	110:22	?	0	298	500	100	[81]

<sup>a</sup>Excess Na<sup>+</sup> or K<sup>+</sup> concentration

<sup>b</sup>Number of lipid molecules with largest mole fraction

<sup>c</sup>Number of water molecules

<sup>d</sup>Number of additional cations

<sup>e</sup>Simulation temperature

<sup>f</sup>Total simulation time

<sup>g</sup>Time used for analysis

<sup>h</sup>Reference for simulation files

<sup>i</sup>Calculation of concentration complicated due the scaled ions. Concentration taken as reported in the delivered data.

<sup>j</sup>Calculation of concentration complicated due the scaled ions. Concentration taken as reported in the delivered data.

terminated by the R-PDLF experiments or calculated from the known  $^2\text{H}$  quadrupolar couplings [7] as input. Chemical shift anisotropy and homonuclear couplings were neglected, and the input file *rep2000* was used to simulate the random distribution of bilayer orientations in the samples studied.

**Sample preparation** The sample was prepared simply by mixing the POPS with water (lipid:water 60:40 wt%) in an eppendorf tube mixing and centrifuging the sample repeatedly until an homogeneous viscous fluid was obtained. 20 mg of sample was then transferred to an NMR insert suitable for 4 mm NMR rotors. **26.Maybe we need little bit more information about the mixing procedure?**

### Molecular dynamics simulations

Molecular dynamics simulation data was collected using the Open Collaboration method [33]. The NMRlipids project blog ([nmrlipids.blogspot.fi](http://nmrlipids.blogspot.fi)) and the GitHub repository ([github.com/NMRLipids/NMRLipidsIVootherHGs](https://github.com/NMRLipids/NMRLipidsIVootherHGs)) were used as the communication platforms. The simulated systems are listed in Tables I (pure PS systems without additional ions) and II (mixed PC:PS systems with various ions concentrations). Simulation details are given in the SI. The simulation data is also indexed in the searchable database ([nmrlipids.fi](http://nmrlipids.fi)), and in the NMRLipids/MATCH GitHub repository (<https://github.com/NMRLipids/MATCH>).

The C-H bond order parameters were calculated directly from the definition

$$S_{\text{CH}} = \frac{1}{2} \langle 3 \cos^2 \theta - 1 \rangle, \quad (1)$$

where  $\theta$  is the angle between the C-H bond and the membrane normal. Angular brackets point to the average over all sampled configurations. The order parameters were first calculated averaging over time separately for each lipid molecule in the system. The average and the standard error of the mean were then calculated over different lipids. The number density profiles were calculated using *gmx density* tool from Gromacs software package [87].

### Comparison of ion binding to negatively charged lipid bilayers between simulations and experiments using the electrometer concept

The order parameters of  $\alpha$  and  $\beta$  carbons in PC lipids can be used to measure the ion binding affinity because they decrease proportionally to the amount of bound positive charge to a bilayer [88–90]. This molecular electrometer concept is especially useful for the comparison between simulations and experiments because the headgroup order parameters can be directly calculated from simulations [34]. Also the headgroup order parameters of negatively charged PS and PG lipids exhibit systemic, but less characterized dependence on

the bound charge [17, 91–93]. Therefore, the ion binding affinity to negatively charged bilayers can be better characterized by measuring the PC headgroup order parameters from mixed bilayers [17, 18, 93], see section S2 in the supplementary information.

Before using the PC headgroup order parameters to quantify the ion binding affinity, it is important to quantify their response to the known amount of bound charge [34, 36]. This can be done using the experimental data from the mixtures of monovalent cationic surfactants (dihexadecyldimethylammonium) and POPC [36, 94], see section S3 in the supplementary information. In this work, we also quantify the response of PC headgroup order parameters to the negatively charged PS headgroups, which also follows the electrometer concept in the experiments [38], see section S2 in the supplementary information.

In the experimental  $^2\text{H}$  NMR literature data used in this work [7, 17], the lipids were first soluted to the buffer and then centrifuged to a pellet which was used in the measurements. Such samples have lower lipid concentration (approximately 10 wt % of lipids [7, 17, 95]) than gravimetric samples (60 wt %) and simulations (approximately 50–60 wt %) in this work. Larger multilamellar repeat distances are expected in the samples with lower lipid concentrations due to the swelling caused by electrostatic repulsion in pure PS lipid systems [96]. However, the PS headgroup order parameters measured from gravimetric sample in this work are in good agreement with the results from centrifuged sample in the literature [7] (Fig. 2). Furthermore, the equilibrium repeat distance rapidly decreases with the addition of monovalent salts and is close to the simulation box sizes already above 500 mM concentrations [96, 97]. Therefore, the hydration levels of multilamellae are expected to be sufficiently similar in the used simulations and reference experiments.

Two different definitions for the salt concentrations have been used when electrometer concept is applied to study ion binding affinity. The concentrations are reported either in water before solvating the lipids [17, 34, 88] or in bulk water after solvating the lipids [36, 89]. In this work, we use the former definition to be consistent with the reference experimental data [17]. The used definition has only a marginal effect to the results in simulations with realistic ion binding affinity (section S4 in the supplementary information).

## RESULTS AND DISCUSSION

### Headgroup and glycerol backbone order parameters of POPS from $^{13}\text{C}$ NMR

The INEPT and 2D R-PDLF experiments from POPS sample give well resolved spectras for all the carbons in headgroup and glycerol backbone region (Fig. 1). The glycerol backbone carbon peaks were assigned according to the POPC spectra [84]. The peaks for  $\beta$  and  $\alpha$  carbons were assigned according to the known order parameters from the  $^2\text{H}$  NMR ex-



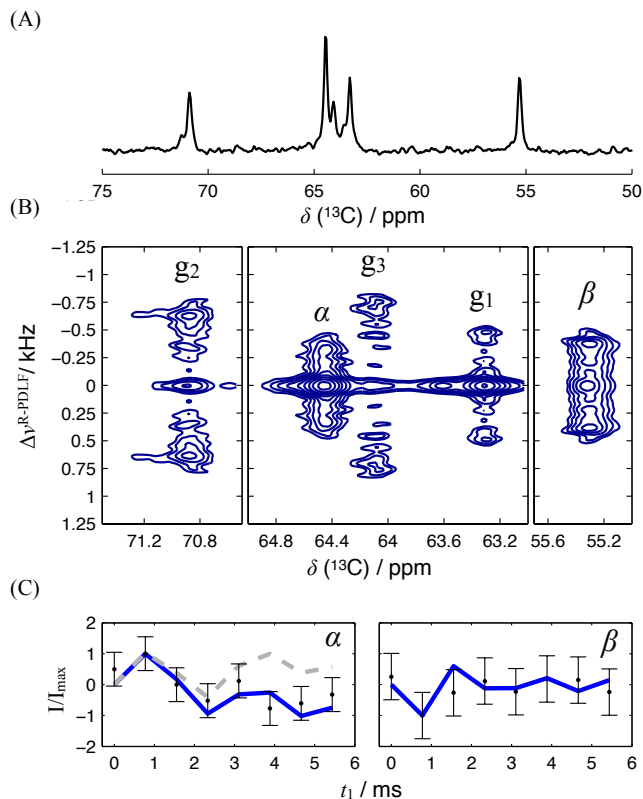


FIG. 1: The headgroup and glycerol backbone region of the (A) INEPT spectrum and (B) 2D R-PDFF spectra. (C) Experimental S-DROSS data (points) and SIMPSON simulations (blue lines) with the order parameter values of -0.12 for the  $\beta$ -carbon, and 0.09 and -0.02 for the  $\alpha$ -carbon slittings. The S-DROSS curve from SIMPSON simulation with positive value for the smaller  $\alpha$ -carbon order parameter (dashed grey).

periments [7]. Slices of the R-PDFF spectra and the resulting order parameters values are shown in the supplementary information (Fig. S6). Since the R-PDFF and previous  $^2\text{H}$  NMR experiments [7, 18] give only the absolute values of order parameters, we determined the signs of PS headgroup order parameters using the S-DROSS experiment [83]. The S-DROSS slice clearly shows that the order parameter of the  $\beta$ -carbon is negative (Fig. 1 C)), which is confirmed by SIMPSON simulations. The beginning of the S-DROSS slice suggests that the larger order parameter of the  $\alpha$ -carbon is positive and the deviation towards negative values with longer  $T_1$  times suggests that the smaller order parameter is negative. This is confirmed by a SIMPSON simulation using the value of -0.02 from  $^2\text{H}$  NMR experiment [18] for the smaller order parameter. The literature value was used because the resolution of our experiment was not sufficient to determine the small value of the order parameter. The S-DROSS curve from SIMPSON simulation with a positive value for the smaller order parameter (dashed grey in Fig. 1 C)) did not agree with the experiment, confirming the interpretation that the smaller order parameter is negative.

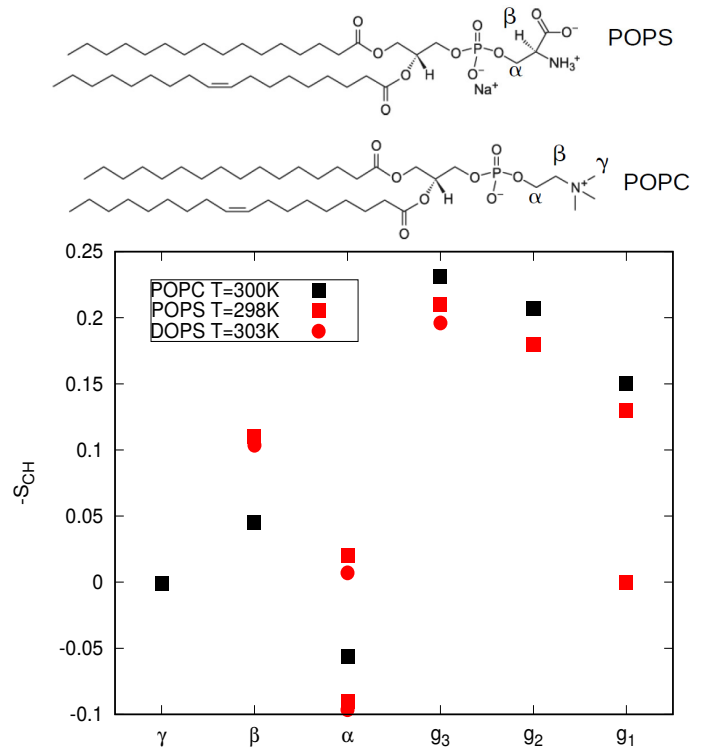


FIG. 2: Headgroup and glycerol backbone order parameters of POPC measured in this work compared with the values from DOPS ( $^2\text{H}$  NMR, 0.1M of NaCl) [7] and POPC ( $^{13}\text{C}$  NMR) [84] experiments. Signs of the PS order parameters are measured in this work. Signs of the PC order parameters are measured in Ref. [85].

The headgroup and glycerol backbone order parameters of POPC measured in this work are in good agreement with the previously reported values from  $^2\text{H}$  NMR experiments of DOPS [7] (Fig. 2). When compared with the previously measured values for POPC [84] (Fig. 2), the  $\beta$ -carbon order parameter is significantly more negative and  $\alpha$ -carbon experiences a significant forking in PS headgroup. These features have been interpreted to arise from a rigid PS headgroup conformation, stabilized by hydrogen bonds or electrostatic interactions [7, 8], but detailed structural interpretation is not available.

#### Headgroup and glycerol backbone in simulations of PS lipid bilayers without additional ions

The headgroup and glycerol backbone of PS lipids show wide variety between different simulation models in the order parameters and structures (Figs. 3 and S9), as previously observed also for PC lipids [33]. The models perform generally less well for PS lipids than for PC lipids in the previous study (Figs. 2 and 4 in Ref. [33] vs. Figs. 3 and 5). Therefore, interpretation of structural differences between PC and PS headgroups from simulations is not straightforward.

The best performing models, Slipids, CHARMM36 and

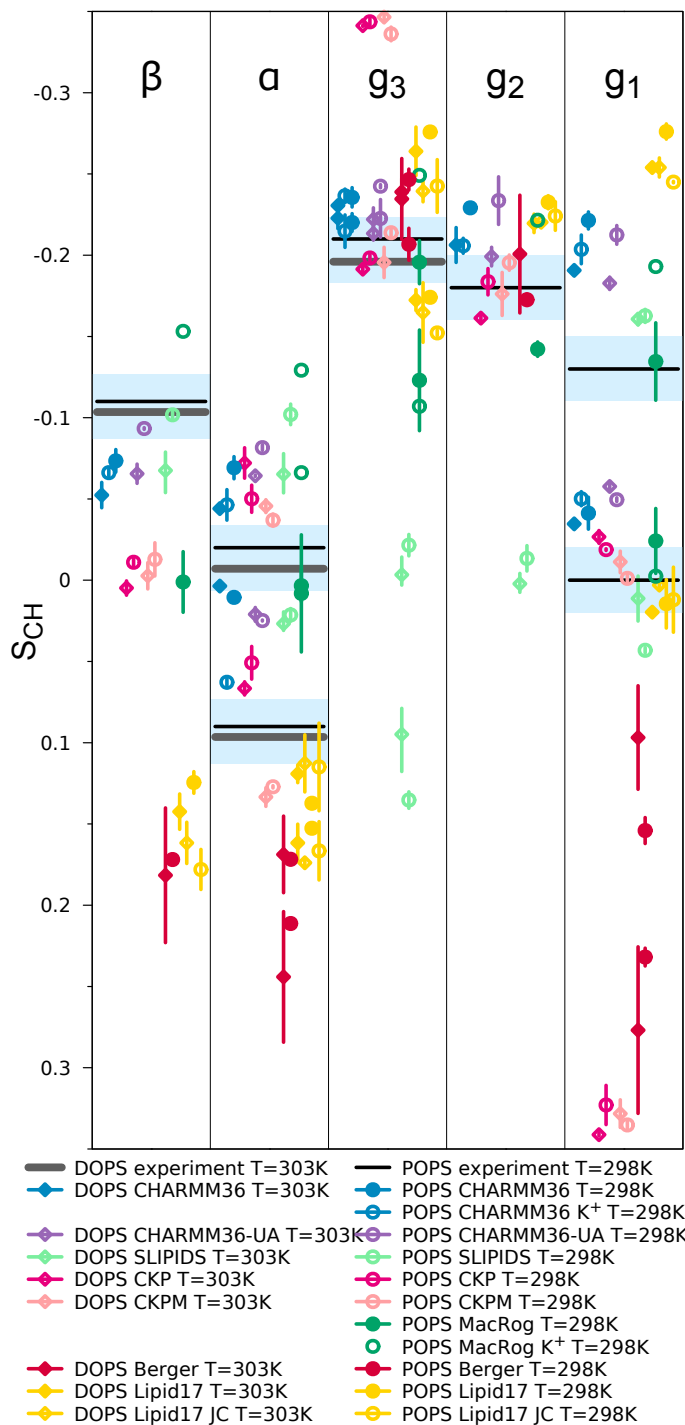


FIG. 3: Order parameters for PS headgroup and glycerol backbone from simulations with different models and experiments without  $\text{CaCl}_2$ . All DOPS data at 303 K, POPS at 298 K. Experimental data from [7] contain 0.1 M of NaCl. Signs are taken from experiments for POPS described in Supplementary Information. The vertical bars shown are not error bars, but demonstrate that we had at least two data sets; the ends of the bars mark the extreme values from the sets, and the dot marks their measurement-time-weighted average.

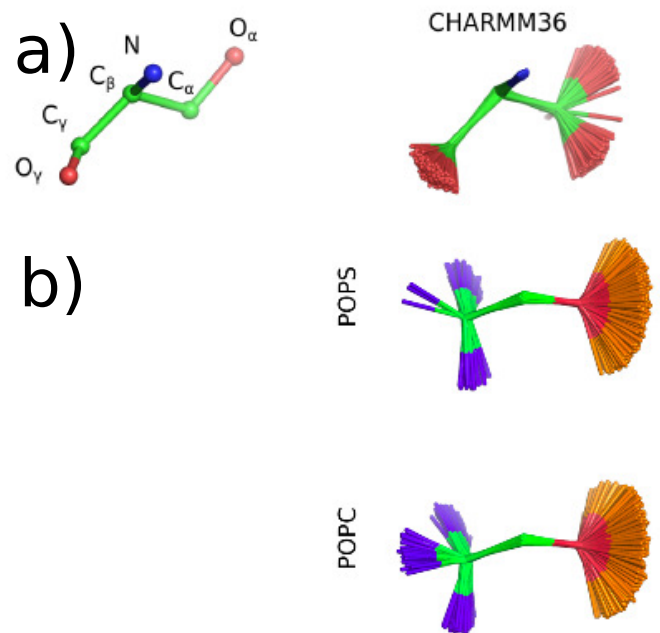


FIG. 4: Overlaid snapshots from glycerol backbone and headgroup region from different simulations of PS lipids.

CHARMM36ua, reproduce the larger forking of the  $\alpha$ -carbon and the Slipids model reproduces also the lower of the  $\beta$ -carbon order parameter when comparing the PS results to PC (Fig. 2 in Ref. 33 vs. Fig. 3). Interestingly, the dihedral angle distributions of  $\text{C}_\alpha\text{-C}_\beta\text{-C}_\gamma\text{-O}_\gamma$  show a single narrow maximum close to  $120^\circ$  in the best three models, while other models give several maxima in different locations (Fig. S7). The restricted motion is also visible in the sampled conformations (Figs. 4 a) and S9) suggesting that the rotation of carboxyl group is limited in the serine headgroup. In addition, the comparison of  $\text{N-C}_\beta\text{-C}_\alpha\text{-O}_\alpha$  dihedral between PC and PS headgroups from CHARMM36 simulations, which are in best agreement with experiments for both lipids, shows a more asymmetric and restricted rotations around this bond (Figs. 4 b) and S10). These results might manifest the increased rigidity anticipated from the early experimental studies [7, 8].

27. Maybe we should move the glycerol backbone results to SI and focus here on the headgroup, and especially to the difference between PC and PS. The glycerol backbone order parameters of  $\text{C}_2$  and  $\text{C}_3$  from Slipids simulations differ significantly from the other simulation results and experiments (Fig. 3), as observed previously also for PC lipids [33]. The origin of this difference is more difficult to track without more elaborate analysis, because different models show very complicated patterns of distinct structures in the glycerol backbone region (Figs. ?? and S7).

	$\beta$	$\alpha$	$g_3$	$g_2$	$g_1$	$\Sigma$
CHARMM 36 K+	M	M	M <sub>F</sub>	M	M <sub>F</sub>	7
CHARMM 36	M	M <sub>F</sub>	M	M	M <sub>F</sub>	8
CHARMM 36-UA	M	M	M	M	M <sub>F</sub>	9
MacRog K+	M	M <sub>F</sub>	M <sub>F</sub>	M	M <sub>F</sub>	11
MacRog	M	M <sub>F</sub>	M <sub>F</sub>	M	M	14
GROMOS-CKP	M	M <sub>F</sub>	M <sub>F</sub>		M <sub>F</sub>	14
GROMOS-CKPM	M	M <sub>F</sub>	M <sub>F</sub>		M <sub>F</sub>	14
Berger	M	M <sub>F</sub>	M <sub>F</sub>		M <sub>F</sub>	14
Slipid	M	M	M <sub>F</sub>	M	M <sub>F</sub>	14
Lipid17	M	M <sub>F</sub>	M <sub>F</sub>	M	M <sub>F</sub>	18
Lipid17 JC	M	M <sub>F</sub>	M <sub>F</sub>	M	M <sub>F</sub>	18

FIG. 5: Rough subjective ranking of force fields based on Figure 3. Here M indicates a magnitude problem, F a forking problem; letter size increases with problem severity. Color scheme: within experimental error (dark green), almost within experimental error (light green), clear deviation from experiments (light red), and major deviation from experiments (dark red). The  $\Sigma$ -column shows the total deviation of the force field, when individual carbons are given weights of 0 (matches experiment), 1, 2, and 4 (major deviation). For full details of the assessment, see Supplementary Information.

#### Counterion binding and interactions between PC and PS headgroups

Membranes containing PS lipids are always accompanied with counterions which modulate electrostatic interactions between lipids and other biomolecules. Counterions are also suggested to screen the repulsion between charged lipid headgroups in MD simulations and reduce the area per lipid of PS bilayers to be smaller than in PC bilayers [23–25]. The counterion density profiles along membrane normal show significant differences between simulation models in both binding affinity and distribution of ions in the interface (Fig. 6).

The experimental area per lipid ( $62.7 \text{ \AA}^2$ ) [30] is reproduced only in Gromos-CKP simulations and in the MacRog simulation with potassium counterions, while other models give significantly lower values (Fig. 6). The counterion binding and concomitant electrostatic screening of the headgroup repulsion does not fully explain the low area per molecule values because the MacRog simulation with strongest sodium binding (the lowest concentrations in bulk water) gives the same area per molecule as CHARMM36ua simulation with significantly weaker counterion binding affinity. On the other hand, changing counterions from sodium to potassium, having weaker binding affinity, increases the area per molecule from  $53 \text{ \AA}^2$  to  $63 \text{ \AA}^2$  in MacRog simulations. In conclusion, the results are in line with the previous study suggesting that the low area per molecule in PS lipid bilayers originate from the combination of both counterion binding and hydrogen bonding network between lipid headgroups [? ].

Binding of coions to zwitterionic PC lipid bilayers has been previously evaluated against experiments using the changes of headgroup order parameters as a function of ion concentration [34]. This is less straightforward for charged lipid bilayers because counterions are always present and the ion free reference state does not exist. In addition, the analysis is complicated by the artificial aggregation of counterions in solution observed in some simulations (section S7 in the supplementary information). Here, we evaluate the amount of bound charge using the changes of headgroup order parameters with increasing amount of negatively charged lipids in the bilayer. According to the electrometer concept, the headgroup order parameters of POPC increase when negatively charged POPS lipids are incorporated in lipid bilayer (section S1) [38, 90]. This is reproduced in the MacRog simulations with potassium counterions having the weakest binding affinity to POPS lipid bilayers (Fig. 6), while other simulations predict no change or decrease in the order parameters (Fig. 7). In Berger and CHARMM36 simulations, the stronger counterion binding cancel the effect of negatively charged headgroups and the headgroup order parameters do not increase with increasing amount of PS lipids. Therefore, we suggest that the relatively weak binding of potassium in the MacRog simulations (Fig. 6) predicts the most realistic surface charge density in membranes containing PS lipids, while the other tested simulation models overestimate the counterion binding affinity. The results are in line with the changes of headgroup order parameters as a function of added counterions analyzed in section S7 in the supplementary information.

The headgroup order parameters of POPS shift closer to zero when bilayer is diluted with POPC (Fig. 7), which is interpreted to indicate less rigid structure of PS headgroups in the mixture [7, 8, 17, 18, 38]. This shift is observed only in lipid14/17 simulations but the numerical values of order parameters are too far from experiments, having also different signs, for the proper interpretation of the experimental data. In CHARMM36 and Gromos-CKP simulations, the shift of headgroup order parameters toward zero are not observed when bilayer diluted with POPC (Fig. 7). Therefore, we conclude

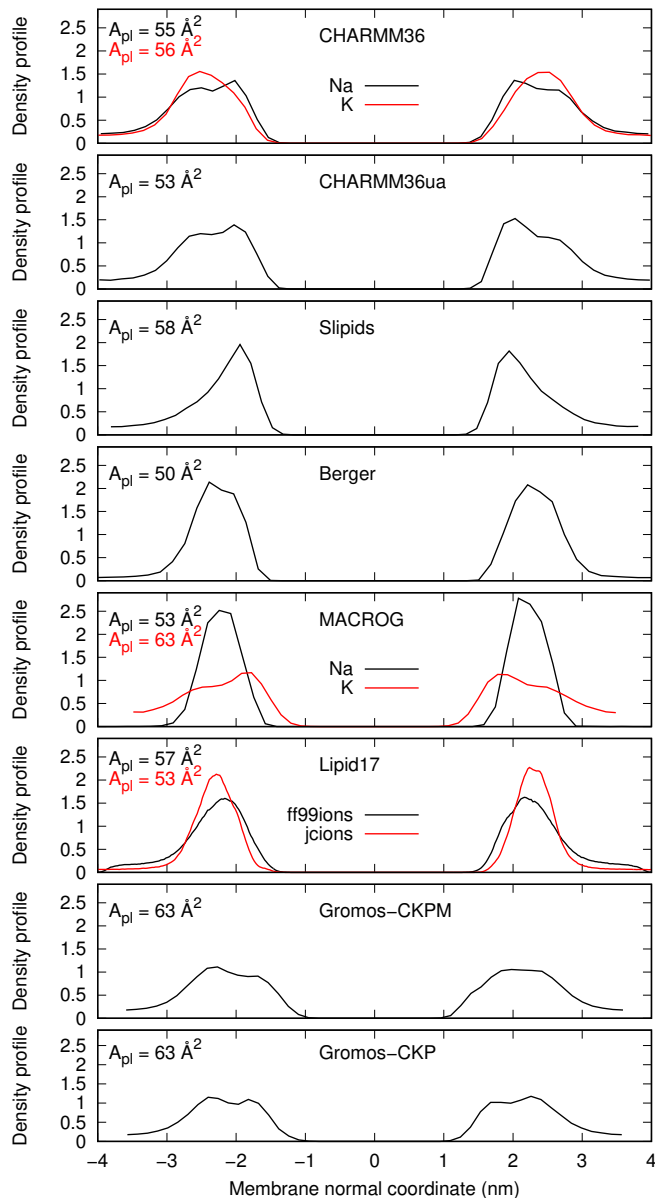


FIG. 6: Counterion densities of POPS lipid bilayer along the membrane normal from simulations with different force fields.

that more accurate force fields are necessary for MD simulation studies of PC-PS headgroup interactions.

### **Ca<sup>2+</sup> binding affinity to bilayers with negatively charged PS lipids**

Ion binding affinity to membranes containing negative charged PS lipids can be measured by detecting the PC lipid headgroup order parameters from POPC:POPS (5:1) mixtures (section S2), where the dehydrated lipid-ion complexes and phase separation are not observed [15–18]. As expected from

the previous study of pure PC lipid bilayers [34], almost all the tested simulation models overestimate the decrease of POPC headgroup order parameters as a function of Ca<sup>2+</sup> concentration in POPC:POPS (5:1) mixtures with respect to the experiments [17] (Fig. 8), indicating overestimated calcium binding affinity. Only exception is the CHARMM36 model with the NBfix interaction employed for calcium [68], which underestimates the order parameter changes indicating weaker binding affinity than experiments. Notably, CHARMM36 simulations with NBfix corrections [29, 68] give similar binding affinities of calcium and sodium to POPC bilayer (see section S8), in contrast to the experimental data [88, 89, 98]. Therefore, we conclude that the calcium binding affinity, manifested by the peaks in the density distributions along membrane normal (Fig. 9), is underestimated in CHARMM36 simulations with the NBfix for calcium [68] but overestimated in all the other tested models.

The headgroup order parameters of POPS measured from POPC:POPS (5:1) mixture exhibit a strong dependence of CaCl<sub>2</sub> with small concentrations and rapid saturation below 100 mM (Fig. 8). The order parameter of POPS  $\beta$ -carbon increase and the larger  $\alpha$ -carbon decrease with the added CaCl<sub>2</sub> in experiments. Slight increase is observed in the smaller  $\alpha$ -carbon. All the changes are significantly overestimated in the tested simulation models, including the CHARMM36 with the NBfix for calcium [68], where the binding affinity was underestimated. In addition, different simulation models predict qualitatively different behaviour for the POPS  $\alpha$ -carbon order parameters with the added calcium. For example, both order parameters decrease in Berger simulations but increase in MacRog simulations, while behaviour in Lipid14/17 and CHARMM36 simulations is more complicated. This is in contrast to the PC headgroup, where qualitatively correct response to the bound ions is observed in all simulation models despite of the significant discrepancies in the headgroup structure without additional ions [34]. Therefore, we conclude that the improvement of force fields is necessary to correctly describe interactions between PS headgroup and calcium ions using MD simulations.

## **CONCLUSIONS**

We have collected a set of experimental NMR order parameter data, which could be combined with MD simulations to interpret the headgroup structure and cation binding details to negatively charged membranes containing PS lipids. Using open collaboration method, we tried to find a MD simulation model which would be sufficiently accurate to interpret the experimental data. However, none of the tested models was accurate enough. In line with the previous study for PC lipids [34], MD simulation models seems to generally overestimate cation binding also to negatively charged bilayers containing PS lipids, with some exceptions. The response of PS lipid headgroup order parameters to the bound cations does not agree with experiments, even in the cases where binding



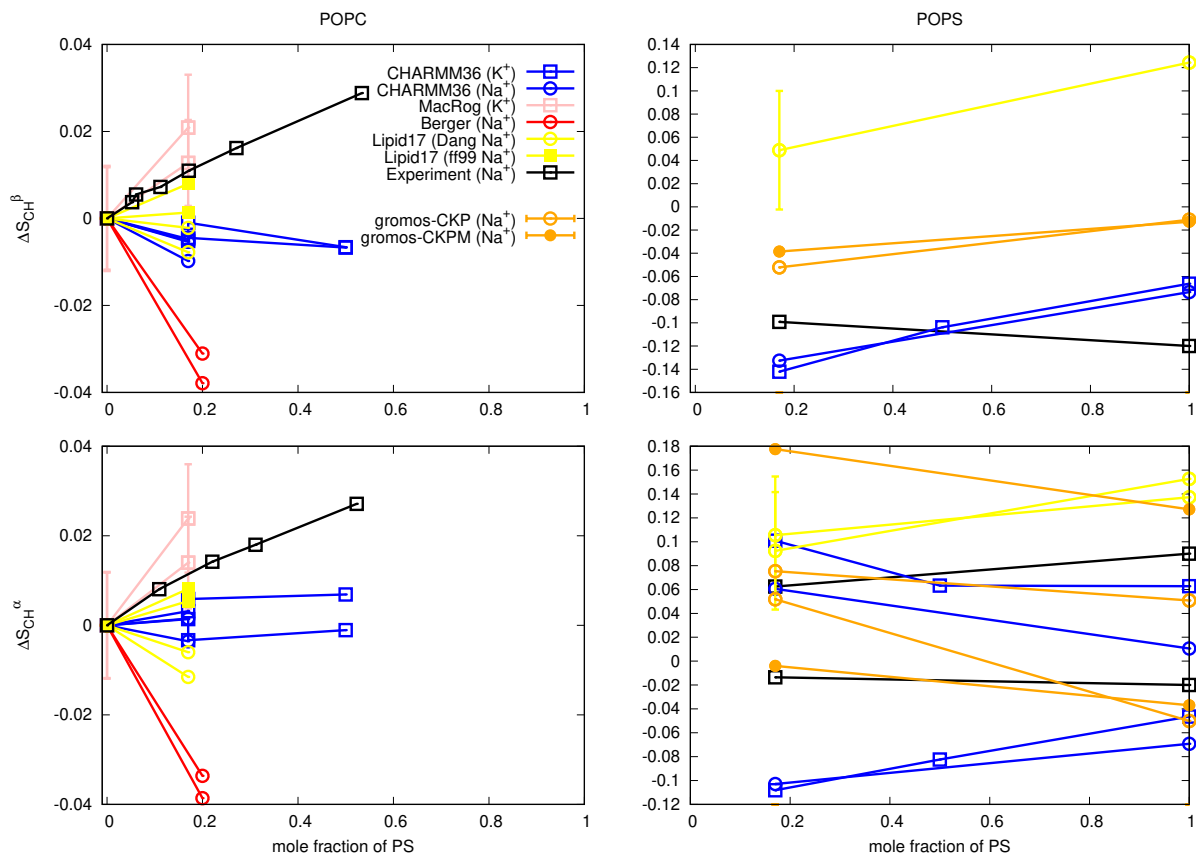


FIG. 7: Changes of PC (left panel) and PS (right panel) headgroup order parameters from POPC:POPS mixtures with increasing amount of POPS. Experimental results of POPC are taken from Ref. 38 (signs are determined as discussed in [33, 35]). Experimental values for POPS in pure bilayer and in mixture are measured in this work and in Ref. 17 at 298K, respectively. Since the experimental data of POPS in pure and diluted mixture come from different experimental sets (13C NMR in this work and 2H NMR from Ref. 17), the experimental change of the order parameter is less accurate than in typical measurements where same technique is used in all conditions, see discussion about qualitative and quantitative accuracy in Ref. 35. For POPC (left panel) the zero point of y-axis is set to the value of pure bilayer. For  $\beta$ -carbon of POPS (right panel, top) the zero point of y-axis is set to the value from POPC:POPS (5:1) mixture. For  $\alpha$ -carbon of POPS (right panel, bottom) the y-axis is transferred with the same value for both order parameters such that the lower order parameter value from POPC:POPS (5:1) mixture is at zero to correctly illustrate the significant forking.

28. Simulation of CHARMM36 at 298K should be maybe rerun with Gromacs 5.

29. The data from POPC used in Gromos-CKP by would be useful for this plot.

affinity is not overestimated. This is in contrast to the previous results with PC lipids, where the qualitative response of the headgroup order parameters was in agreement with experiments even in the cases where the headgroup structure without ions was not correct and the cation binding affinity was overestimated. In addition, the inaccurate responses of PS headgroup order parameters to the dilution with PC lipids suggests that the PC-PS interactions are not accurately described by the tested models.

Our results pave the way for improving the PS lipid parameters for MD simulations by offering the set of experimental data for the quality measurement, by pinpointing problems areas in the models and suggesting directions for the corrections. Improvements using the electronic continuum correction is already in progress [https://github.com/jmelcr/ecc\\_lipids](https://github.com/jmelcr/ecc_lipids), following the recent work for PC

lipids [36].

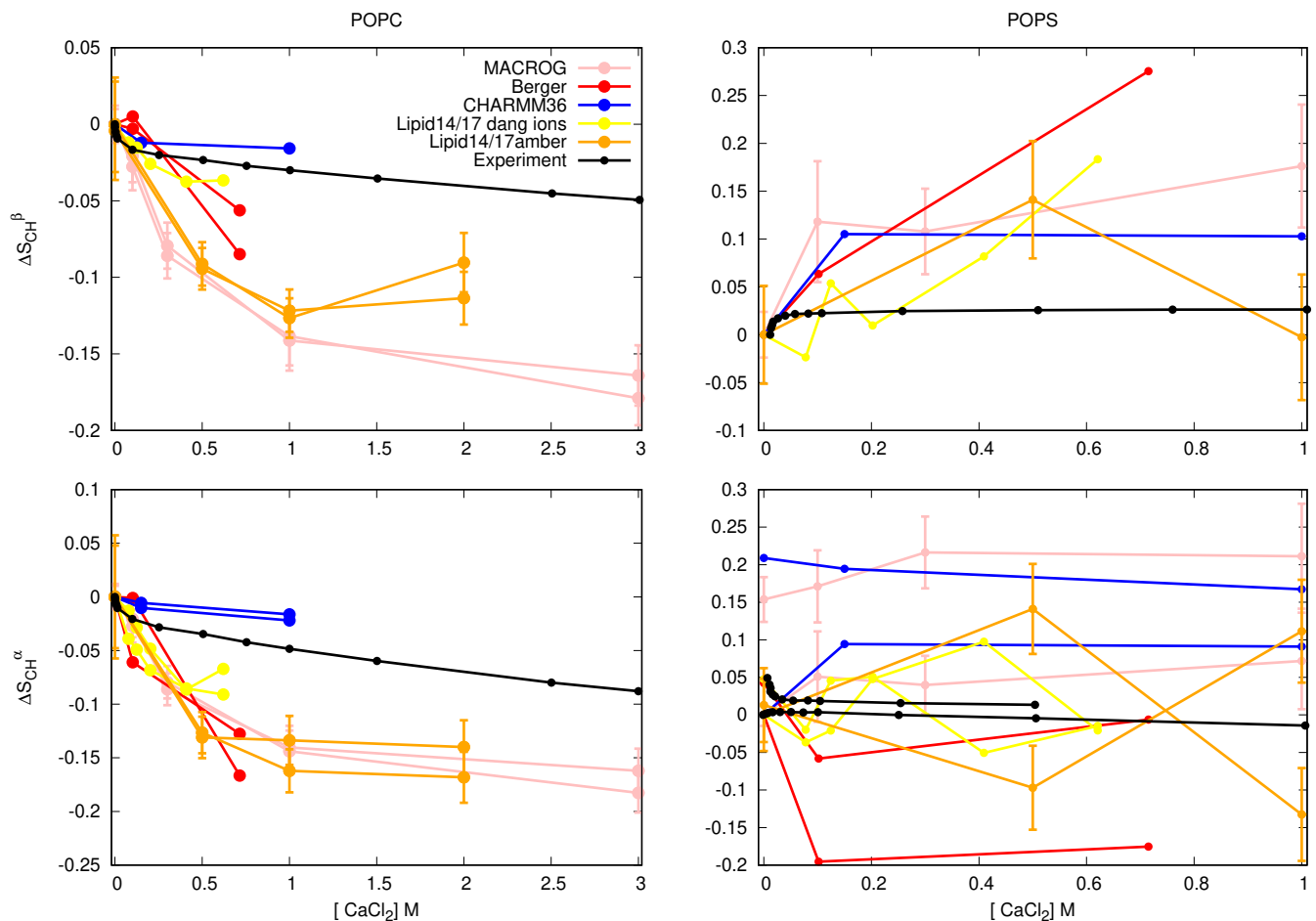


FIG. 8: Changes of POPC (left) and POPS (right) headgroup order parameters from POPC:POPS (5:1) mixture as a function  $\text{CaCl}_2$  concentration from experiments 17 and different simulations at 298K (except the data for Berger model is from simulation of POPC:POPS (4:1) mixture at 310K [32, 99]). The order parameter values from systems without calcium are set as the zero point of y-axis, except for the  $\alpha$ -carbon order parameter of POPS (bottom, right) for which the both order parameters are shifted such that the lower order parameter is zero without additional ions to correctly illustrate the forking with different concentrations of calcium. Potassium counterions are used in MacRog simulations and sodium counterions in Lipid14/17 simulations. In CHARMM36 and Berger simulation with added calcium, the charge is neutralized with calcium and monovalent counterions are not present.

30.Upcoming simulations with original CHARMM36 have been mentioned in the blog:

<http://nmrlipids.blogspot.com/2017/12/nmrlipids-iv-current-status-and.html?showComment=1520090718976#c5569269391707740056>

\* samuli.ollila@helsinki.fi

- [1] M. A. Lemmon, Nat. Rev. Mol. Cell Biol. **9**, 99 (2008).
- [2] P. A. Leventis and S. Grinstein, Annual Review of Biophysics **39**, 407 (2010).
- [3] L. Li, X. Shi, X. Guo, H. Li, and C. Xu, Trends in Biochemical Sciences **39**, 130 (2014), ISSN 0968-0004.
- [4] T. Yeung, G. E. Gilbert, J. Shi, J. Silvius, A. Kapus, and S. Grinstein, Science **319**, 210 (2008).
- [5] H. Zhao, E. K. J. Tuominen, and P. K. J. Kinnunen, Biochemistry **43**, 10302 (2004).
- [6] G. P. Gorbenko and P. K. Kinnunen, Chemistry and Physics of Lipids **141**, 72 (2006).
- [7] J. L. Browning and J. Seelig, Biochemistry **19**, 1262 (1980).
- [8] G. Büdlt and R. Wohlgemuth, The Journal of Membrane Biology **58**, 81 (1981), ISSN 1432-1424, URL <http://dx.doi.org/10.1007/BF01870972>.
- [9] H. Hauser, E. Finer, and A. Darke, Biochemical and Biophysical Research Communications **76**, 267 (1977), ISSN 0006-291X, URL <http://www.sciencedirect.com/science/article/pii/0006291X77907215>.
- [10] R. J. Kurland, Biochemical and Biophysical Research Communications **88**, 927 (1979), ISSN 0006-291X, URL <http://www.sciencedirect.com/science/article/pii/0006291X79914979>.
- [11] M. Eisenberg, T. Gresalfi, T. Riccio, and S. McLaughlin, Biochemistry **18**, 5213 (1979).
- [12] H. Hauser and G. G. Shipley, Biochemistry **22**, 2171 (1983).
- [13] R. Dluhy, D. G. Cameron, H. H. Mantsch, and R. Mendelsohn, Biochemistry **22**, 6318 (1983).

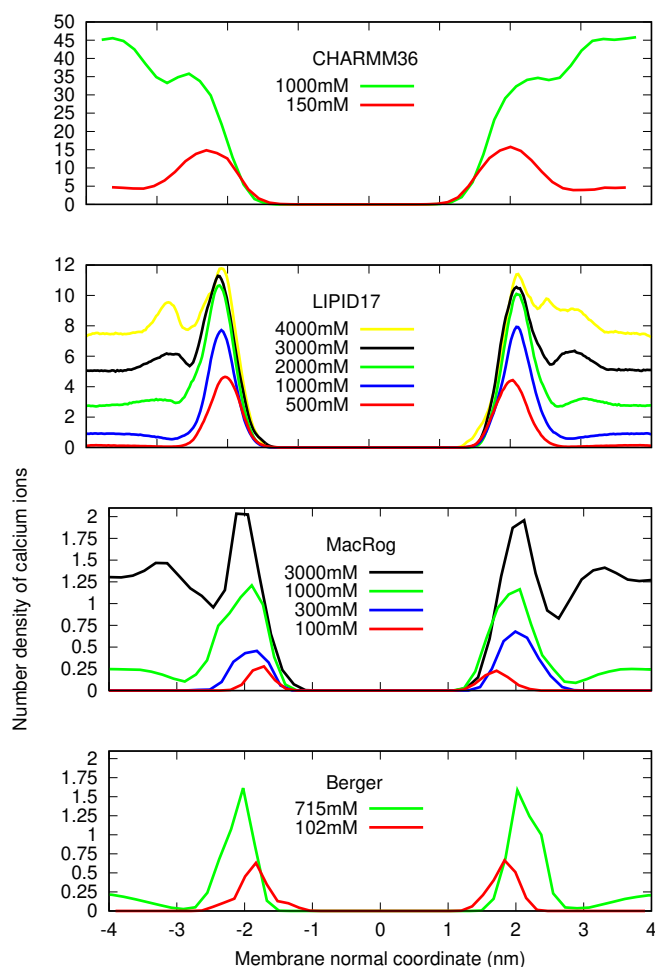


FIG. 9:  $\text{Ca}^{2+}$  density profiles from simulations.

31. The CHARMM results are mass densities, number densities should be used when the data by Jesper Madsen is available.

32. Should we include also counterions into the plot?

33. Figure needs general improvement.

[14] H. Hauser and G. Shipley, *Biochimica et Biophysica Acta (BBA) - Biomembranes* **813**, 343 (1985), ISSN 0005-2736, URL <http://www.sciencedirect.com/science/article/pii/0005273685902512>.  
 [15] G. W. Feigenson, *Biochemistry* **25**, 5819 (1986).  
 [16] J. Mattai, H. Hauser, R. A. Demel, and G. G. Shipley, *Biochemistry* **28**, 2322 (1989).  
 [17] M. Roux and M. Bloom, *Biochemistry* **29**, 7077 (1990).  
 [18] M. Roux and M. Bloom, *Biophys. J.* **60**, 38 (1991).  
 [19] J. M. Boettcher, R. L. Davis-Harrison, M. C. Clay, A. J. Nieuwkoop, Y. Z. Ohkubo, E. Tajkhorshid, J. H. Morrissey, and C. M. Rienstra, *Biochemistry* **50**, 2264 (2011).  
 [20] J. Seelig, *Cell Biology International Reports* **14**, 353 (1990), ISSN 0309-1651, URL <http://www.sciencedirect.com/science/article/pii/030916519091204H>.  
 [21] C. G. Sinn, M. Antonietti, and R. Dimova, *Colloids and Sur-*

faces A: Physicochemical and Engineering Aspects **282-283**, 410 (2006), a Collection of Papers in Honor of Professor Ivan B. Ivanov (Laboratory of Chemical Physics and Engineering, University of Sofia) Celebrating his Contributions to Colloid and Surface Science on the Occasion of his 70th Birthday.  
 [22] J. J. Lpez Cascales, J. Garca de la Torre, S. J. Marrink, and H. J. C. Berendsen, *The Journal of Chemical Physics* **104**, 2713 (1996).  
 [23] S. A. Pandit and M. L. Berkowitz, *Biophysical Journal* **82**, 1818 (2002).  
 [24] P. Mukhopadhyay, L. Monticelli, and D. P. Tieleman, *Biophysical Journal* **86**, 1601 (2004).  
 [25] U. R. Pedersen, C. Leidy, P. Westh, and G. H. Peters, *Biochimica et Biophysica Acta (BBA) - Biomembranes* **1758**, 573 (2006).  
 [26] P. T. Vernier, M. J. Ziegler, and R. Dimova, *Langmuir* **25**, 1020 (2009).  
 [27] A. Martn-Molina, C. Rodrguez-Beas, and J. Faraudo, *Biophysical Journal* **102**, 2095 (2012).  
 [28] P. Jurkiewicz, L. Cwiklik, A. Vojtkov, P. Jungwirth, and M. Hof, *Biochimica et Biophysica Acta (BBA) - Biomembranes* **1818**, 609 (2012).  
 [29] R. M. Venable, Y. Luo, K. Gawrisch, B. Roux, and R. W. Pastor, *The Journal of Physical Chemistry B* **117**, 10183 (2013).  
 [30] J. Pan, X. Cheng, L. Monticelli, F. A. Heberle, N. Kucerka, D. P. Tieleman, and J. Katsaras, *Soft Matter* **10**, 3716 (2014).  
 [31] S. Vangaveti and A. Travesset, *The Journal of Chemical Physics* **141**, 245102 (2014).  
 [32] A. Melcrová, S. Pokorna, S. Pullanchery, M. Kohagen, P. Jurkiewicz, M. Hof, P. Jungwirth, P. S. Cremer, and L. Cwiklik, *Sci. Reports* **6**, 38035 (2016).  
 [33] A. Botan, F. Favela-Rosales, P. F. J. Fuchs, M. Javanainen, M. Kandu, W. Kulig, A. Lamberg, C. Loison, A. Lyubartsev, M. S. Miettinen, et al., *J. Phys. Chem. B* **119**, 15075 (2015).  
 [34] A. Catte, M. Girych, M. Javanainen, C. Loison, J. Melcr, M. S. Miettinen, L. Monticelli, J. Maatta, V. S. Oganessian, O. H. S. Ollila, et al., *Phys. Chem. Chem. Phys.* **18**, 32560 (2016).  
 [35] O. S. Ollila and G. Pabst, *Biochimica et Biophysica Acta (BBA) - Biomembranes* **1858**, 2512 (2016).  
 [36] J. Melcr, H. Martinez-Seara, R. Nencini, J. Kolafa, P. Jungwirth, and O. H. S. Ollila, *The Journal of Physical Chemistry B* **122**, 4546 (2018).  
 [37] H. U. Gally, G. Pluschke, P. Overath, and J. Seelig, *Biochemistry* **20**, 1826 (1981).  
 [38] P. Scherer and J. Seelig, *EMBO J.* **6** (1987).  
 [39] T. Piggot, *CHARMM36 DOPS simulations (versions 1 and 2) 303 K 1.0 nm LJ switching* (2017), URL <https://doi.org/10.5281/zenodo.1129411>.  
 [40] T. Piggot, *CHARMM36-UA DOPS simulations (versions 1 and 2) 303 K 1.0 nm LJ switching* (2017), URL <https://doi.org/10.5281/zenodo.1129456>.  
 [41] J. P. M. Jämbeck and A. P. Lyubartsev, *Phys. Chem. Chem. Phys.* **15**, 4677 (2013).  
 [42] T. Piggot, *Slipids DOPS simulations (versions 1 and 2) 303 K 1.0 nm cut-off with LJ-PME* (2017), URL <https://doi.org/10.5281/zenodo.1129439>.  
 [43] F. Favela-Rosales, *MD simulation trajectory of a fully hydrated DOPS bilayer: SLIPIDS, Gromacs 5.0.4. 2017.* (2017), URL <https://doi.org/10.5281/zenodo.495510>.  
 [44] T. Piggot, *Berger DOPS simulations (versions 1 and 2) 303 K 1.0 nm cut-off* (2017), URL <https://doi.org/10.5281/zenodo.1129419>.  
 [45] T. Piggot, *GROMOS-CKP DOPS simulations (versions 1 and 2) 303 K with Berger/Chiu NH3 charges and PME* (2017), URL

- <https://doi.org/10.5281/zenodo.1129429>.
- [46] T. Piggot, *GROMOS-CKP DOPS simulations (versions 1 and 2) 303 K with GROMOS NH3 charges and PME* (2017), URL <https://doi.org/10.5281/zenodo.1129447>.
  - [47] I. Gould, A. Skjevik, C. Dickson, B. Madej, and R. Walker, *Lipid17: A comprehensive amber force field for the simulation of zwitterionic and anionic lipids* (2018), in preparation.
  - [48] I. S. Joung and T. E. Cheatham, *The Journal of Physical Chemistry B* **112**, 9020 (2008).
  - [49] B. Kav and M. S. Miettinen, *Molecular dynamics simulation trajectory of an anionic lipid bilayer: 100 mol% DOPS with Na+ counterions using Joung-Cheatham Ions* (2018), B.K acknowledges financial support from International Max Planck Research School on Multiscale Bio-Systems, URL <https://doi.org/10.5281/zenodo.1134871>.
  - [50] J. Åqvist, *J. Phys. Chem.* **94**, 8021 (1990).
  - [51] B. Kav and M. S. Miettinen, *Molecular dynamics simulation trajectory of an anionic lipid bilayer: 100 mol% DOPS with Na+ counterions using ff99 Ions* (2018), B.K acknowledges financial support from International Max Planck Research School on Multiscale Bio-Systems, URL <https://doi.org/10.5281/zenodo.1135142>.
  - [52] T. Piggot, *CHARMM36 POPS simulations (versions 1 and 2) 298 K 1.0 nm LJ switching* (2017), URL <https://doi.org/10.5281/zenodo.1129415>.
  - [53] T. Piggot, *CHARMM36 POPS simulations (versions 1 and 2) 298 K 1.0 nm LJ switching with K ions* (2018), URL <https://doi.org/10.5281/zenodo.1182654>.
  - [54] T. Piggot, *CHARMM36-UA POPS simulations (versions 1 and 2) 298 K 1.0 nm LJ switching* (2017), URL <https://doi.org/10.5281/zenodo.1129458>.
  - [55] T. Piggot, *Slipids POPS simulations (versions 1 and 2) 298 K 1.0 nm cut-off with LJ-PME* (2017), URL <https://doi.org/10.5281/zenodo.1129441>.
  - [56] T. Piggot, *Berger POPS simulations (versions 1 and 2) 298 K 1.0 nm cut-off* (2017), URL <https://doi.org/10.5281/zenodo.1129425>.
  - [57] A. Maciejewski, M. Pasenkiewicz-Gierula, O. Cramariuc, I. Vattulainen, and T. Róg, *J. Phys. Chem. B* **118**, 4571 (2014).
  - [58] T. Piggot, *MacRog POPS simulations (versions 1 and 2) 298 K with corrected PO not OP tails* (2018), URL <https://doi.org/10.5281/zenodo.1283335>.
  - [59] M. Javanainen, *Simulation of a pops bilayer* (2017), URL <https://doi.org/10.5281/zenodo.1120287>.
  - [60] T. Piggot, *GROMOS-CKP POPS simulations (versions 1 and 2) 298 K with Berger/Chiu NH3 charges and PME* (2017), URL <https://doi.org/10.5281/zenodo.1129431>.
  - [61] T. Piggot, *GROMOS-CKP POPS simulations (versions 1 and 2) 298 K with GROMOS NH3 charges and PME* (2017), URL <https://doi.org/10.5281/zenodo.1129435>.
  - [62] M. S. Miettinen and B. Kav, *Molecular dynamics simulation trajectory of an anionic lipid bilayer: 100 mol% POPS with Na+ counterions using Joung-Cheatham Ions* (2018), B.K. acknowledges financial support from International Max Planck Research School on Multiscale Bio-Systems., URL <https://doi.org/10.5281/zenodo.1148495>.
  - [63] M. S. Miettinen and B. Kav, *Molecular dynamics simulation trajectory of an anionic lipid bilayer: 100 mol% POPS with Na+ counterions using ff99 ions* (2018), B.K. acknowledges financial support from International Max Planck Research School on Multiscale Bio-Systems, URL <https://doi.org/10.5281/zenodo.1134869>.
  - [64] J. B. Klauda, R. M. Venable, J. A. Freites, J. W. O'Connor, D. J. Tobias, C. Mondragon-Ramirez, I. Vorobyov, A. D. MacKerell Jr, and R. W. Pastor, *J. Phys. Chem. B* **114**, 7830 (2010).
  - [65] O. H. S. Ollila, *POPS+83%popc lipid bilayer simulation at T298K ran CHARMM\_GUI force field and Gromacs* (2017), URL <https://doi.org/10.5281/zenodo.1011104>.
  - [66] T. Piggot, *CHARMM36 POPS/POPC simulations (versions 1 and 2) 298 K 1.0 nm LJ switching with K ions* (2018), URL <https://doi.org/10.5281/zenodo.1182658>.
  - [67] T. Piggot, *CHARMM36 POPS/POPC simulations (versions 1 and 2) 298 K 1.0 nm LJ switching with Na ions* (2018), URL <https://doi.org/10.5281/zenodo.1182665>.
  - [68] S. Kim, D. Patel, S. Park, J. Slusky, J. Klauda, G. Widmalm, and W. Im, *Biophysical Journal* **111**, 1750 (2016), ISSN 0006-3495, URL <http://www.sciencedirect.com/science/article/pii/S0006349516307615>.
  - [69] M. Javanainen, *Simulations of popc/pops membranes with cacl2*. (2017), URL <https://doi.org/10.5281/zenodo.1409551>.
  - [70] M. Javanainen, *Simulations of popc/pops membranes with kcl* (2018), URL <https://doi.org/10.5281/zenodo.1404040>.
  - [71] C. J. Dickson, B. D. Madej, A. A. Skjevik, R. M. Betz, K. Teigen, I. R. Gould, and R. C. Walker, *J. Chem. Theory Comput.* **10**, 865 (2014).
  - [72] B. Kav and M. S. Miettinen, *Amber Lipid17 Simulations of POPC/POPS Membranes with KCl Counterions* (2018), B.K acknowledges financial support from International Max Planck Research School on Multiscale Bio-Systems, URL <https://doi.org/10.5281/zenodo.1250969>.
  - [73] B. Kav and M. S. Miettinen, *Amber Lipid17 Simulations of POPC/POPS Membranes with KCl* (2018), B.K acknowledges financial support from International Max Planck Research School on Multiscale Bio-Systems, URL <https://doi.org/10.5281/zenodo.1227257>.
  - [74] B. Kav and M. S. Miettinen, *Amber Lipid17 Simulations of POPC/POPS Membranes with NaCl Counterions* (2018), B.K acknowledges financial support from International Max Planck Research School on Multiscale Bio-Systems, URL <https://doi.org/10.5281/zenodo.1250975>.
  - [75] B. Kav and M. S. Miettinen, *Amber Lipid17 Simulations of POPC/POPS Membranes with NaCl* (2018), B.K acknowledges financial support from International Max Planck Research School on Multiscale Bio-Systems, URL <https://doi.org/10.5281/zenodo.1227272>.
  - [76] D. P. Tieleman, H. J. Berendsen, and M. S. Sansom, *Biophys. J.* **76**, 1757 (1999).
  - [77] L. Cwiklik, *MD simulation trajectory of a POPC/POPS (4:1) bilayer with 1M NaCl, Berger force field for lipids and ffmx for ions* (2017), URL <https://doi.org/10.5281/zenodo.838219>.
  - [78] C. Lukasz, *MD simulation trajectory of a POPC/POPS (4:1) bilayer with 102mM CaCl2, Berger force field for lipids, scaled charges for Ca2+ and Cl-* (2017), URL <https://doi.org/10.5281/zenodo.887398>.
  - [79] C. Lukasz, *MD simulation trajectory of a POPC/POPS (4:1) bilayer with 715mM CaCl2, Berger force field for lipids, scaled charges for Ca2+ and Cl-* (2017), URL <https://doi.org/10.5281/zenodo.887400>.
  - [80] T. Piggot, *GROMOS-CKP POPS/POPC simulations (versions 1 and 2) 298 K with GROMOS NH3 charges and PME* (2018), URL <https://doi.org/10.5281/zenodo.1283333>.
  - [81] T. Piggot, *GROMOS-CKP POPS/POPC simulations (versions 1 and 2) 298 K with Berger/Chiu NH3 charges*

- and *PME* (2018), URL <https://doi.org/10.5281/zenodo.1283331>.
- [82] S. V. Dvinskikh, H. Zimmermann, A. Maliniak, and D. Sandstrom, *J. Magn. Reson.* **168**, 194 (2004).
- [83] J. D. Gross, D. E. Warschawski, and R. G. Griffin, *J. Am. Chem. Soc.* **119**, 796 (1997).
- [84] T. M. Ferreira, F. Coreta-Gomes, O. H. S. Ollila, M. J. Moreno, W. L. C. Vaz, and D. Topgaard, *Phys. Chem. Chem. Phys.* **15**, 1976 (2013).
- [85] T. M. Ferreira, R. Sood, R. Bärenwald, G. Carlström, D. Topgaard, K. Saalwächter, P. K. J. Kinnunen, and O. H. S. Ollila, *Langmuir* **32**, 6524 (2016).
- [86] M. Bak, J. T. Rasmussen, and N. C. Nielsen, *Journal of Magnetic Resonance* **147**, 296 (2000), ISSN 1090-7807, URL <http://www.sciencedirect.com/science/article/pii/S1090780700921797>.
- [87] M. Abraham, D. van der Spoel, E. Lindahl, B. Hess, and the GROMACS development team, *GROMACS user manual version 5.0.7* (2015), URL [www.gromacs.org](http://www.gromacs.org).
- [88] H. Akutsu and J. Seelig, *Biochemistry* **20**, 7366 (1981).
- [89] C. Altenbach and J. Seelig, *Biochemistry* **23**, 3913 (1984).
- [90] J. Seelig, P. M. MacDonald, and P. G. Scherer, *Biochemistry* **26**, 7535 (1987).
- [91] F. Borle and J. Seelig, *Chemistry and Physics of Lipids* **36**, 263 (1985).
- [92] P. M. Macdonald and J. Seelig, *Biochemistry* **26**, 1231 (1987).
- [93] M. Roux and J.-M. Neumann, *FEBS Letters* **199**, 33 (1986).
- [94] P. G. Scherer and J. Seelig, *Biochemistry* **28**, 7720 (1989).
- [95] M. Roux, J.-M. Neumann, M. Bloom, and P. F. Devaux, *European Biophysics Journal* **16**, 267 (1988).
- [96] M. Loosley-Millman, R. Rand, and V. Parsegian, *Biophysical Journal* **40**, 221 (1982).
- [97] R. Rand and V. Parsegian, *Biochimica et Biophysica Acta (BBA) - Reviews on Biomembranes* **988**, 351 (1989).
- [98] G. Cevc, *Biochim. Biophys. Acta - Rev. Biomemb.* **1031**, 311 (1990).
- [99] S. Ollila, M. T. Hyvönen, and I. Vattulainen, *J. Phys. Chem. B* **111**, 3139 (2007).

### ToDo

- |  | P. |
|--|----|
| 1. Authorlist is not yet complete . . . . .  | 1  |
| 2. Correct citation for CHARMMua DOPS . . . . .  | 2  |
| 3. Correct citation(s) for CKP. . . . .  | 2  |
| 4. Correct citation(s) for CKP. . . . .  | 2  |
| 5. Correct citation for CHARMMua DOPS . . . . .  | 2  |
| 6. Correct citation(s) for CKP. . . . .  | 2  |
| 7. Correct citation(s) for CKP. . . . .  | 2  |
| 8. Equilibration? . . . . .  | 3  |
| 9. Trajectories and further details to be added by J. Madsen . . . . .   | 3  |
| 10. Concentration to be checked after the amount of water molecules is known. . . . .  | 3  |
| 11. Trajectories and further details to be added by J. Madsen . . . . .  | 3  |
| 12. Concentration to be checked after the amount of water molecules is known. . . . .  | 3  |
| 13. Trajectories and further details to be added by J. Madsen . . . . .  | 3  |
| 14. Trajectories and further details to be added by J. Madsen . . . . .  | 3  |
| 15. Concentration to be checked after the amount of ions is known. . . . .   | 3  |
| 16. Concentration to be checked after the amount of ions is known. . . . .   | 3  |
| 17. Concentration to be checked after the amount of ions is known. . . . .   | 3  |
| 18. Concentration to be checked after the amount of ions is known. . . . .   | 3  |
| 19. Concentration to be checked after the amount of ions is known. . . . .   | 3  |
| 20. Concentration to be checked after the amount of ions is known. . . . .   | 3  |
| 21. Concentration to be checked after the amount of ions is known. . . . .   | 3  |
| 22. Concentration to be checked after the amount of ions is known. . . . .   | 3  |
| 23. Concentration to be checked after the amount of ions is known. . . . .   | 3  |
| 24. Concentration to be checked after the amount of ions is known. . . . .   | 3  |
| 25. Are these correct references? . . . . .  | 3  |
| 26. Maybe we need little bit more information about the mixing procedure? . . . . .  | 4  |
| 27. Maybe we should move the glycerol backbone results to SI and focus here on the headgroup, and especially to the difference between PC and PS. . . . .  | 6  |
| 28. Simulation of CHARMM36 at 298K should be maybe rerun with Gromacs 5. . . . .   | 9  |
| 29. The data from POPC used in Gromos-CKP by would be useful for this plot. . . . .  | 9  |
| 30. Upcoming simulations with original CHARMM36 have been mentioned in the blog: <a href="http://nmrlipids.blogspot.com/2017/12/nmrlipids-iv-current-status-and.html?showComment=1520090718976#c55692693">http://nmrlipids.blogspot.com/2017/12/nmrlipids-iv-current-status-and.html?showComment=1520090718976#c55692693</a> |    |
| 31. The CHARMM results are mass densities, number densities should be used when the data by Jesper Madsen is available. . . . .  | 11 |
| 32. Should we include also counterions into the plot? . . . . .  | 11 |
| 33. Figure needs general improvement. . . . .  | 11 |